*36th EPS Conference on Plasma Phys. Sofia, June 29 - July 3, 2009 ECA Vol.**33E**, O-5.055 (2009)*

Pedestal characteristics of ELMy H-mode plasmas in JT-60U

H. Urano, Y. Sakamoto, N. Oyama, K. Kamiya, A. Kojima, N. Hayashi, N. Aiba,

Y. Kamada and JT-60 Team

Japan Atomic Energy Agency, Naka Fusion Institute, 311-0193, Naka, Japan

1. Introduction

Predicting the edge pedestal structure remains an outstanding issue for burning plasma machines such as ITER because the edge pedestal structure determines the boundary condition of the heat transport of the plasma core and strongly affects the ELM activity. In order to understand the physics of the ELM trigger and determining the ELM size, understanding the pedestal characteristics is of primary importance. In JT-60U, the pedestal characteristics have intensively been studied for the type-I ELMy H-mode and alternative operation modes of small/no ELMs.

ELMs are periodic fast collapse which brings a large heat load to divertor and first wall. Particularly, the characteristics of type-I ELMs are important because large amplitude of these ELMs can be dangerous to the plasma facing components while the type-I ELMy H-mode has a wide operational space and favourable confinement. On the other hand, grassy ELMy H-mode and quiescent H-mode are categorized in H-mode with mitigated or suppressed ELMs which are beneficial to protecting from large heat load onto the diverter plate. However, the operational areas of these ELMy H-modes are limited compared to that of conventional type-I ELMy H-mode. Therefore, understanding the characteristics of these small ELMs is of primary importance to extend those operational areas. The structure of the H-mode pedestal is composed of a spatial width in which a steep pressure gradient is formed. In this region, the periodic expulsion of energy and particles is commonly observed due to the existence of ELMs caused by a steep pressure gradient or a large bootstrap current. However, the dependence of the pedestal width Δ_{ped} on local plasma parameters is not

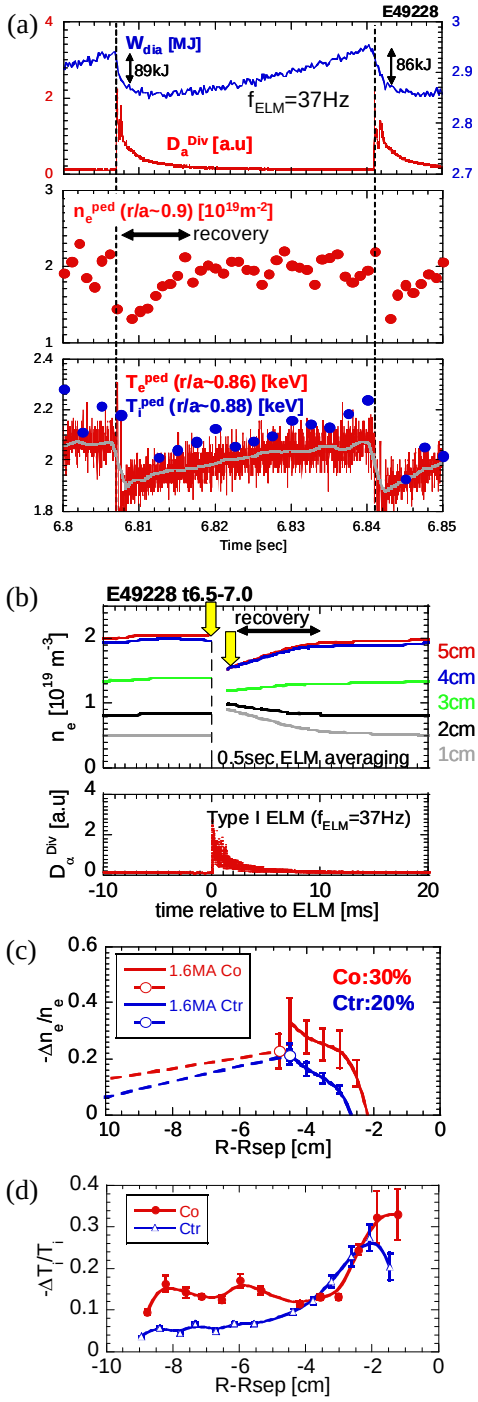

Figure 1. (a) Time evolution of plasma parameters during type-I ELMy H-mode phase. (b) Changes in the edge electron density with a type-I ELM crash. ELM affected profiles of (c) n_e and (d) T_i for the cases with co and counter-NBI.

clearly known. Particularly, knowledge of Δ_{ped} based on non-dimensional parameters is of great help for the extrapolation towards next step device. In this paper, the type-I ELM dynamics, small ELM characteristics of grassy and QH-mode and dimensionless parameter dependence of pedestal width are reported as a recent progress of JT-60U pedestal study.

2. Type-I ELM dynamics

In JT-60U, it has been observed that type-I ELM activity depends sensitively on the edge toroidal rotation [1]. Higher ELM frequency $\boldsymbol{f}_{ELM}$ and smaller ELM energy loss ΔW_{ELM} were observed with increasing the toroidal rotation in counter even at a given power crossing the separatrix. In case of co-NBI, ELM frequency is lower and drop of edge electron temperature profile measured with the fast ECE diagnostics becomes larger. In addition, ELM affected area also extends more inward in case of co-NBI. Recently, behaviors of edge $\boldsymbol{n}_e$ and $\boldsymbol{T}_i$ were measured during an ELM cycle using fast LiBP and CXRS diagnostics [2]. Shown in Fig. 1(a) is a time evolution of the pedestal top values of $\boldsymbol{n}_e$, $\boldsymbol{T}_e$ and $\boldsymbol{T}_i$. After the ELM crash, $\boldsymbol{T}_e$ and $\boldsymbol{T}_i$ increase gradually until the next ELM occurs. On the other hand, the recovery of pedestal density of about 10ms occurs faster than that of temperature. Then, pedestal density is almost fixed or slightly increased. Fig. 1(b) shows a change of $\boldsymbol{n}_e$ in the edge steep gradient region during ELMs. As you can see, there exists a pivot inside the separatrix. The separatrix density is increased by the rapidly enhanced particle flux due to ELM crash. Using fast $\boldsymbol{n}_e$ and $\boldsymbol{T}_i$ measurements, the ELM perturbation profiles can be compared between co and counter-NBI. Figs. 1(c) and (d) show the ELM affected area of electron density and ion temperature. For both cases, ELM affected area extends inward at co-NBI similarly to the electron temperature.

3. Small ELM operation regime of grassy and quiescent H-mode

Since the ELM energy loss of type-I ELM can cause a large heat load onto the divertor plate, several ELM mitigation or ELM suppression techniques have widely been studied. Among many methods proposed and intensively studied, JT-60 dedicated to understanding and extending the small ELM regime of grassy and QH-mode plasmas.

Grassy ELM generally has high frequency at hundred to thousand Hz. In these couple of

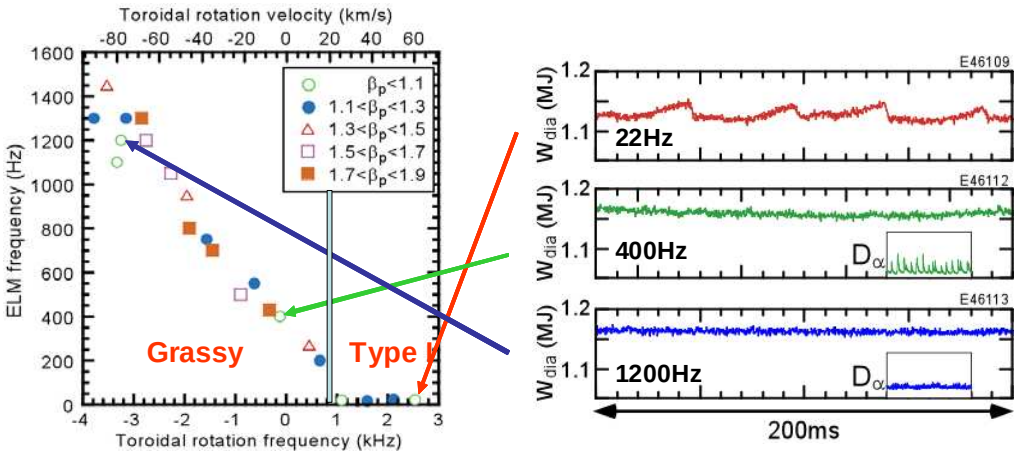

Figure 2. Relation between ELM frequency and toroidal rotation in type-I and grassy ELMs. Time evolutions of plasma stored energy for the cases of toroidal rotation in co, balanced and counter.

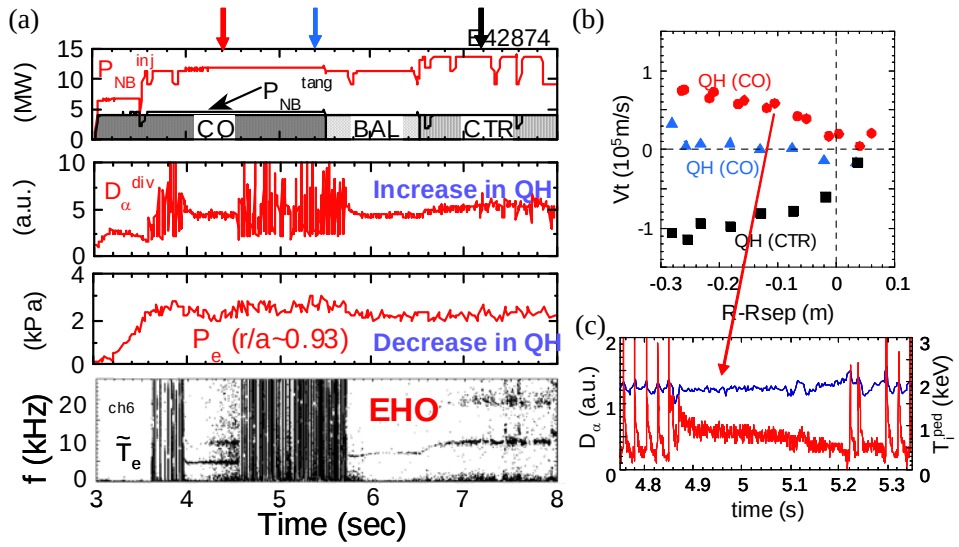

Figure 3. (a) Time evolution of plasma parameters during the QH-mode discharge: $\boldsymbol{P}_{NB}^{inj}$: NB injection power, D_α^{div}: D_α emission intensity in the divertor region, $\boldsymbol{P}_e$: electron pressure at the pedestal top, $\boldsymbol{f}$: fluctuation frequency measured with ECE at the pedestal top. (b) Profiles of toroidal rotation velocity. Triangles and squares correspond to the QH-mode plasmas with co and counter-NBs. Circles are the data in the QH-mode plasma in case where toroidal rotation goes in co-direction at the plasma edge (c) D_α emission signal and $\boldsymbol{T}_i$ at the pedestal top for the case indicated by circles in Fig. 3(b).

years, it was found that grassy ELM frequency depends on the toroidal rotation [3]. At nearly zero rotation, grassy ELM frequency becomes about 400 Hz (see Fig. 2). When the counter rotation is increased, ELM frequency is linearly increased independently of β_p. However, grassy ELM with the frequency of 400 Hz at nearly zero toroidal rotation shows no detectable loss in $\boldsymbol{W}_{dia}$ because of very narrow radial extent of collapse. In this case, ELM energy loss is already less than 1% of the pedestal energy and is an acceptable level in ITER. Recently, it is found that behavior of grassy ELM is changed by the edge collisionality ν^*. In high safety factor case ($\boldsymbol{q}_{95} > 6$), pure grassy ELMs were obtained for both cases of low and high ν^*. When the ν^* is increased, large amplitude of ELM spike with smaller ELM frequency is observed, but this is still not detectable loss of energy in $\boldsymbol{W}_{dia}$. In low safety factor case ($\boldsymbol{q}_{95} \sim 4.2$), mixture of grassy and type-I ELMs is observed. At higher ν^*, frequency of type-I ELMs becomes higher and amplitude of grassy ELM spike becomes larger. These results suggest that the amplitude of grassy ELM decreases as edge ν^* decreases, which is opposite ν^* dependence from type I ELM.

QH-mode has generally been observed in low density plasmas with a large clearance (> 10cm) and the counter torque input. In the recent experiment performed in JT-60U, QH-mode phase was obtained without counter-NB and at nearly zero or slightly co-toroidal rotation at the plasma edge. Fig. 3(a) shows the time evolution of rotation scan in ELMy H-mode plasmas. During the discharge, the direction of tangential NB was changed. Then, in case of balance to counter beam, since the edge toroidal rotation became in counter, QH-mode phase appeared. During QH-mode phase, pedestal pressure becomes lower by 10-20% than type-I ELM. Edge harmonic oscillation (EHO) localized at pedestal may enhance the edge transport. In this discharge, QH-mode phase was observed in co-NBI phase. As shown by the triangles in Fig. 3(b), toroidal rotation at the plasma edge is still in counter [4]. The perpendicular NBs added to the co-tangential NB enhanced the counter rotation the

plasma edge. However, in the other experiment where the toroidal rotation profile is in co-direction for whole range of plasma (see circles in Fig. 3(b)), QH-mode phase was obtained at nearly zero or slightly co-toroidal rotation at the plasma edge.

4. Dimensionless parameter dependence of pedestal width

While several empirical scalings of pedestal width Δ_{ped} have been proposed, these scalings are different from machine to machine. This disagreement can be caused by the existing strong co-linearity between ρ* and β, which is hard to separate out due to the existence of ELM stability limit of edge pressure. To distinguish these variables, a pair of experiments in hydrogen and deuterium plasmas are conducted in JT-60U. Explicit difference between ρ* and β is the mass dependence of ρ* ($\propto \boldsymbol{m}^{0.5}$) in contrast with no mass dependence in β. The investigation of the mass dependence of the pedestal width can reveal the dependence of Δ_{ped} on the edge non-dimensional parameters.

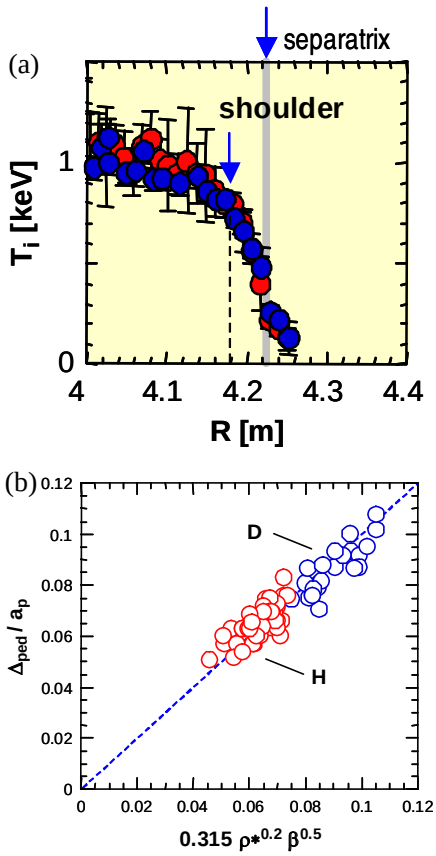

Figure 4. (a) Pedestal $\boldsymbol{T}_i$ profiles for deuterium and hydrogen plasmas at the same β and ν*. (b) Scaling of H-mode pedestal width obtained by dimensionless transport experiment.

The experiments were conducted at fixed $\boldsymbol{B}_T$ = 2.4T, κ = 1.4, δ = 0.34 and ε = 0.27 for deuterium and hydrogen discharges. To keep a sufficient range of ρ* and β value, a set of discharges was performed with different $\boldsymbol{I}_p$ = 0.90, 1.08 and 1.25MA, each of which were tuned by varying the NB injection power $\boldsymbol{P}_{NB}$ so that β can be matched for both species. At matched β between hydrogen and deuterium plasmas, the required power in the hydrogen plasma is ~ 2 times larger than that in deuterium plasma. As seen in figure 4(a), the edge $\boldsymbol{T}_i$ profiles are obviously almost identical for both cases. Considering the fact that ρ* values are different by the square root of mass ratio, ρ* dependence on Δ_{ped} is weak. Figure 4(b) shows the scaling of Δ_{ped} ($\propto \boldsymbol{a}_p$ $\rho^{*0.2}$ $\beta^{0.5}$) obtained in this experiment [5]. A strong correlation between β and ρ* was clearly separated. This result of weak ρ* dependence of pedestal width is favorable in ITER. This is because ρ* is expected to be smaller in ITER due to the increased machine size than that in the present tokamaks.

References

[1] H. Urano, et al., Nucl. Fusion **47** (2007) 706
[2] A. Kojima, et al., submitted to Nucl. Fusion.
[3] N. Oyama, et al., Plasma Phys. Control. Fusion **49** (2007) 249
[4] Y. Sakamoto et al., Plasma Phys. Control. Fusion 46 (2004) A299
[5] H. Urano, et al., Nucl. Fusion **48** (2008) 045008